

Current Biology, Volume 21

Supplemental Information

Temporal Control of Contractile Ring

Assembly by Plo1 Regulation of Myosin II

Recruitment by Mid1/Anillin

Maria Almonacid, Séverine Celton-Morizur, Jennifer L. Jakubowski, Florent Dingli, Damarys Loew, Adeline Mayeux, Jun-Song Chen, Kathleen L. Gould, Dawn M. Clifford, and Anne Paoletti

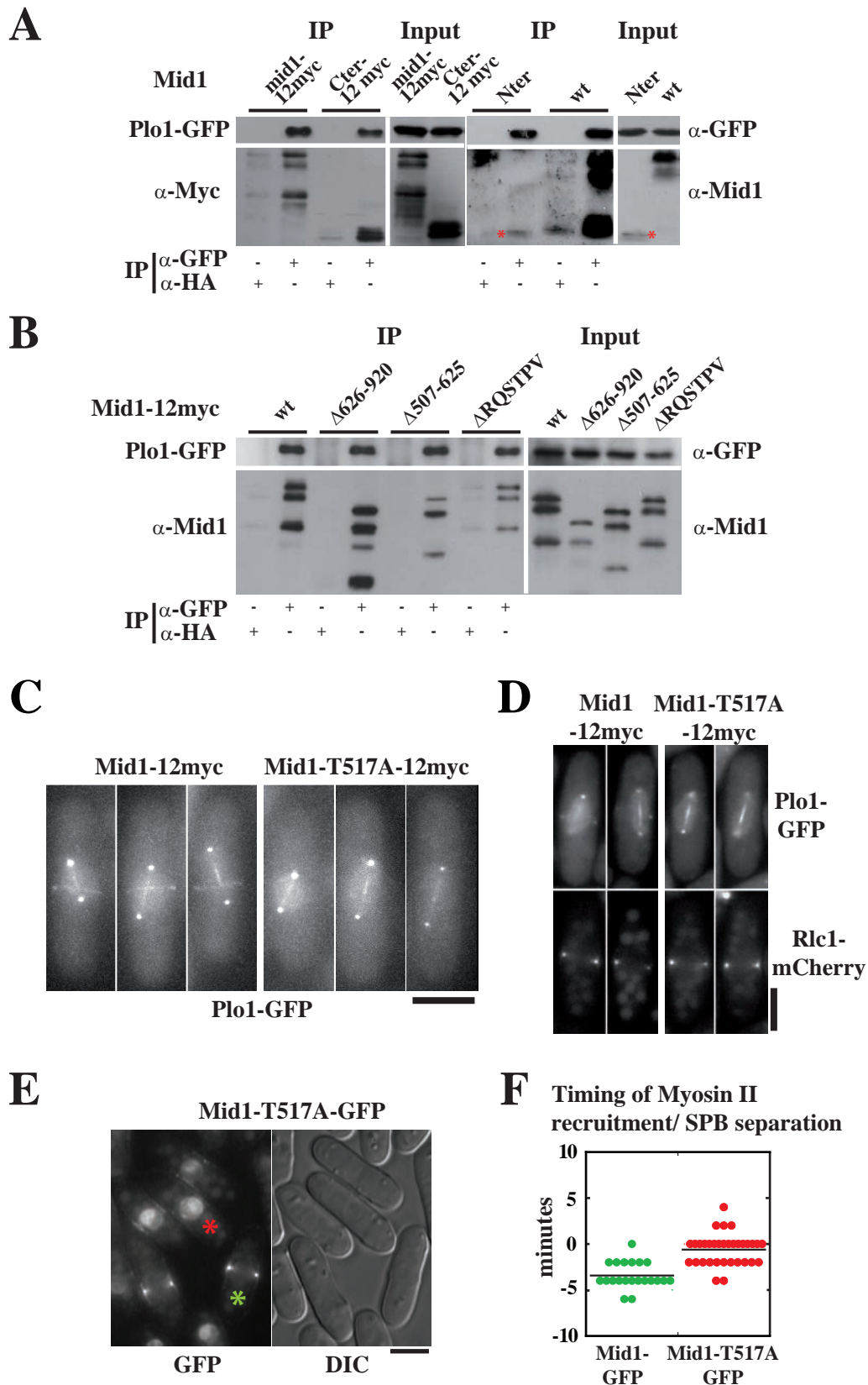


Figure S1: Role of the C-terminal consensus site RQSTPV in Plo1-binding to Mid1

A-B: Immunoprecipitation between Plo1-GFP and Mid1 constructs expressed in *mid1Δ* cells. IPs and WB for Plo1-GFP were performed with an anti-GFP mAb. Mid1 constructs were detected using anti-Mid1 affinity purified Ab (α-Mid1) or an anti-myc mAb. Negative controls: anti-HA IP on same extracts. Red stars highlight the weakly expressed Mid1 Nter. **C:** Localization of Plo1-GFP in *mid1Δ* cells expressing Mid1-12myc (left) or Mid1-T517A-12myc (right) in early mitosis. Maximum projection of z stacks. Bar: 5 μm. **D:** Localization of Plo1-GFP (top) and Rlc1-mCherry (bottom) in *mid1Δ* cells expressing Mid1-12myc (left) or Mid1-T517A-12myc (right) in early mitosis. Bar: 5 μm. **E:** Localization of Mid1-T517A-GFP in *mid1Δ* cells. Bar: 5 μm. Red star: interphase cell with nuclear and medial cortex staining. Green star: mitotic cell with well compacted contractile ring and no nuclear staining. **F:** Timing of Rlc1-mcherry cortical recruitment in cells deleted for *mid1* expressing Mid1-GFP (green) or Mid1-T517A-GFP (red), Rlc1-mcherry and SPB component SfilmRFP as a marker for mitosis entry. Student t-test P value <10⁻⁷. Mid1-GFP: n=21. Mid1-T517A-GFP: n=33.

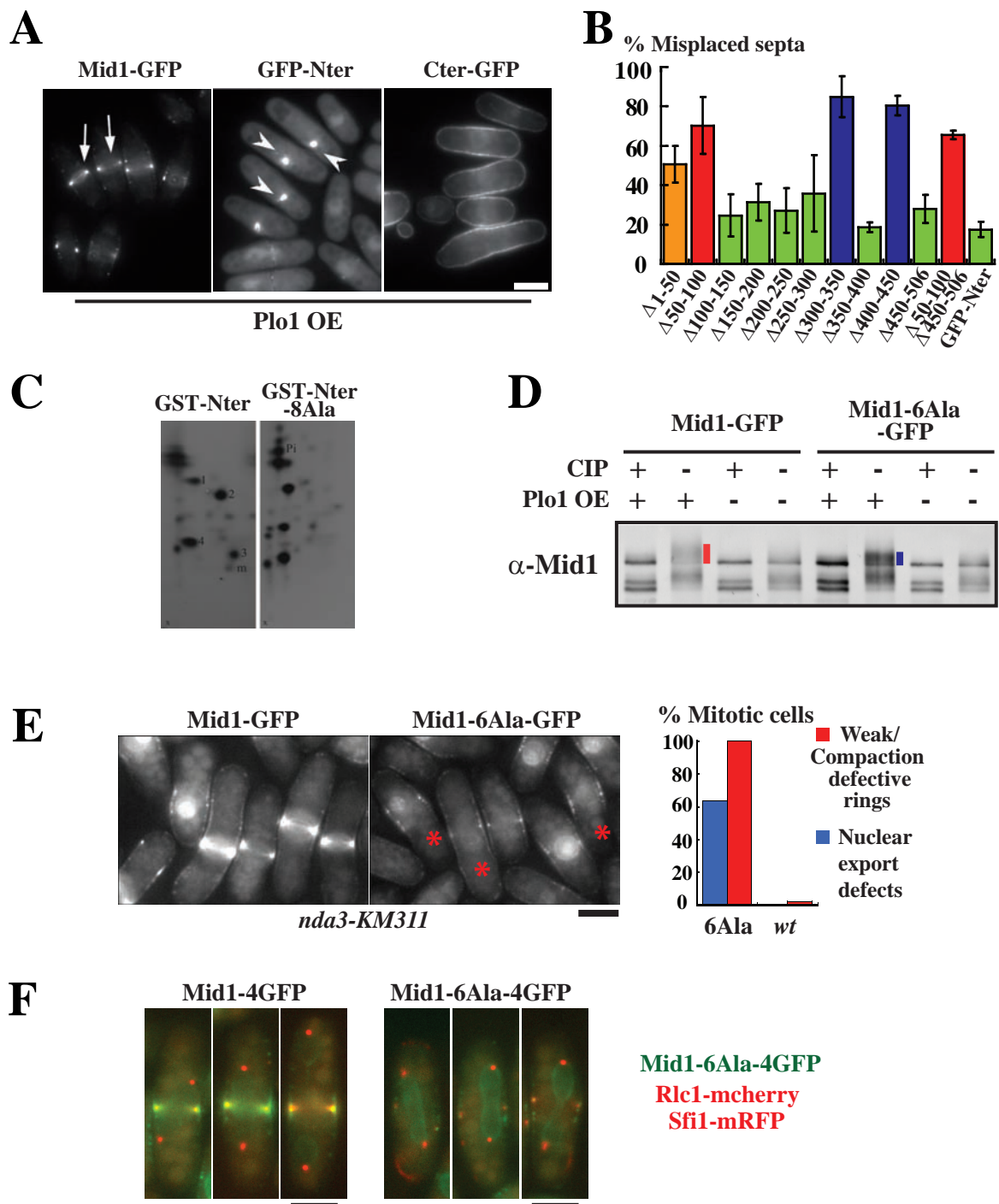


Figure S2: Plo1 overexpression effects and analysis of phospho-defective mutants

A: Plo1 overexpression for 22 hours at room temperature in *mid1Δ* cells expressing Mid1-GFP, GFP-Nter (Mid1 aa 1-506) or Cter-GFP (aa 500-920). Arrows point out ectopic Mid1-GFP cortical rings in interphase and arrowheads filamentous clusters of Mid1 GFP-Nter. Bar: 4 μm. **B:** Percentage of misplaced septa in *mid1Δ* cells expressing Mid1 Nter deletion constructs. Mutants with strong phenotypes are shown in orange and red except cortex anchoring mutants, shown in blue. Cells were grown at 30°C. Error bars : SD, 9 independent counts of 100 cells. **C:** Two-dimensional phospho-tryptic peptide analysis of Mid1 GST-Nter and Mid1 GST-Nter-8Ala phosphorylated by Plo1 kinase. Positions of four major phospho-tryptic peptides are shown. In Mid1 GST-Nter-8Ala, two major (2=S24 and 3=T34) and a minor phosphopeptide (m=S15) are eliminated while phosphorylation of a minor site is enhanced. X indicates origin. The anode is on the left. **D:** Migration patterns of Mid1-GFP and Mid1-6Ala-GFP upon Plo1 overexpression for 22 hours at 25°C. Mid1-GFP and Mid1-6Ala-GFP were immunoprecipitated using an anti-GFP mAb and treated or not with CIP. Mid1 was detected with anti-Mid1 affinity purified Ab (α-Mid1). Red and blue bars outline the mobility shifts upon Plo1 overexpression. **E:** Localization of Mid1-GFP (left) and Mid1-6Ala-GFP (right) in *nda3-KM311* cells blocked in mitosis for 6 hours at 18°C. Stars point out cells with incomplete nuclear export of Mid1-6Ala and defects in compaction of Mid1-6Ala into a tight ring. Bar: 5 μm. Right: Percentage mitotic cells with nuclear export defects and weak rings or ring compaction defects. **F:** Localization of Mid1-4GFP (left) and Mid1-6Ala-4GFP (right) during anaphase. Mid1 is shown in green and Rlc1-mcherry and the SPB marker Sfi1-mRFP are shown in red. Bar: 4 μm.

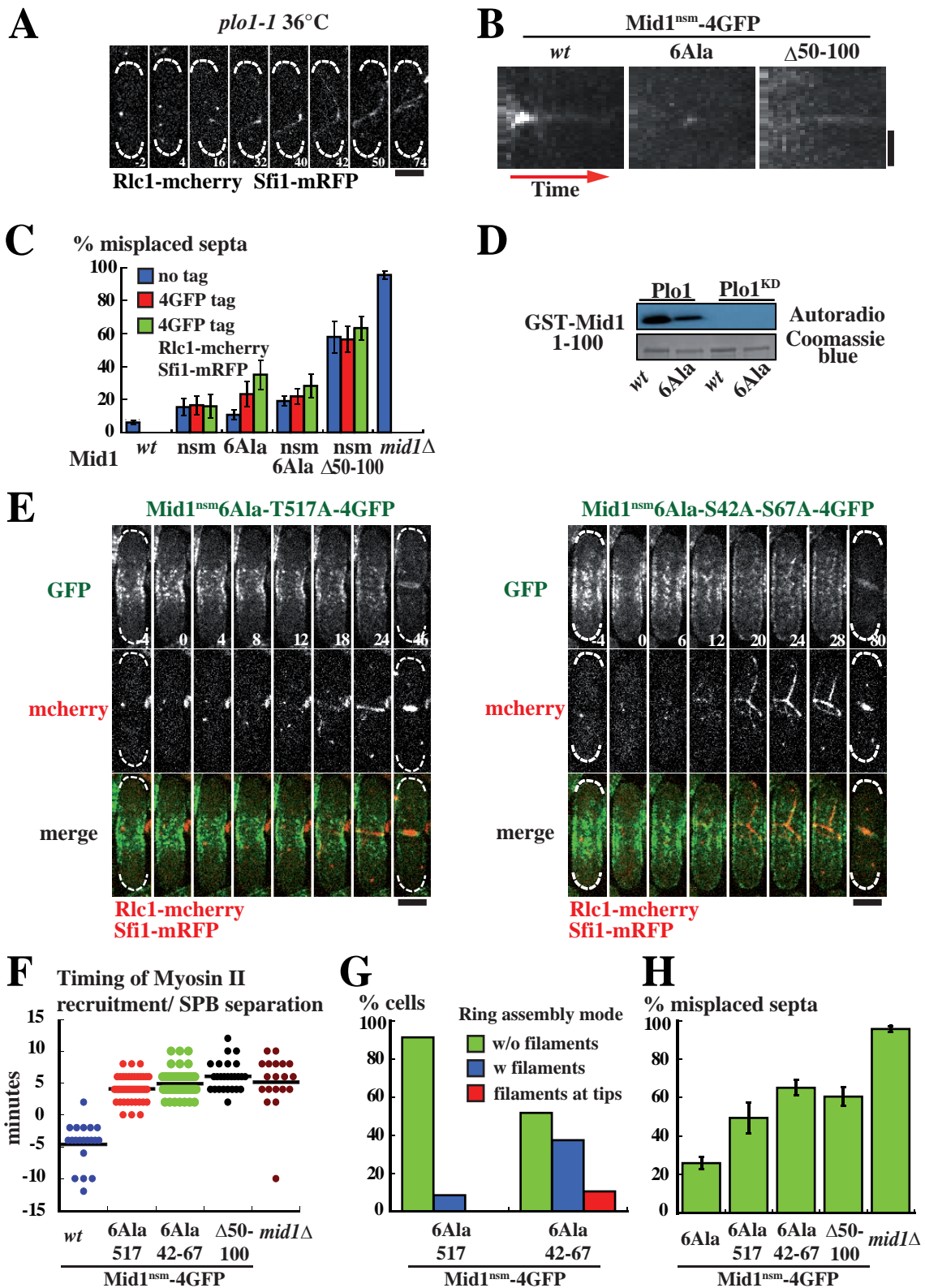


Figure S3: Myosin II recruitment and septum position in *plc1-1* and Mid1 phospho-defective mutants.

A: Time-lapse movie of *plc1-1* mutant expressing Rlc1-mcherry and SPB component Sfi1-mRFP at 36°C. Time is in minutes. Time 0: SPB separation. Bar: 4 μm **B:** Kymographs of GFP fluorescence at the medial cortex over time in Mid1^{nsm}-4GFP, Mid1^{nsm}6Ala-4GFP and Mid1^{nsm}Δ50-100-4GFP cells shown in Fig3A. 1 pixel/4 minutes. Bar: 2 μm. **C:** Percentage of misplaced septa in cells expressing untagged or 4GFP tagged Mid1 mutants. Cells were grown at 30°C. Error bars: SD, 6 independent counts of 100 cells. **D:** Plo1 kinase assay on Mid1 1-100 and Mid1 1-100-6Ala fragments. Phosphorylation is detected by ³²P autoradiography (top). Loading control: coomassie blue staining of GST-Mid1 1-100 and GST-Mid1 1-100 -6Ala (bottom). Negative control: kinase assay with kinase dead Plo1 (KD). **E:** Time-lapse movies of cells expressing Mid1^{nsm}6Ala-T517A-4GFP (A) or Mid1^{nsm}6Ala-S42A-S67A-4GFP (A), Rlc1-mcherry and SPB component Sfi1-mRFP. Mid1 is shown in green and Rlc1 and Sfi1 in red. Time is in minutes. Time 0: SPB separation. Bar: 4 μm. **F:** Timing of Rlc1-mcherry cortical recruitment. wt: n=20. Mid1^{nsm}6Ala-T517A-4GFP: n=47. Mid1^{nsm}6Ala-S42A-S67A-4GFP: n=52. Mid1^{nsm}Δ50-100-4GFP: n=26. *mid1*Δ cells: n=19. **G:** Contractile ring assembly mode. Green: without filaments, blue: with filaments, red: with filaments starting at tips. Mid1^{nsm}6Ala-T517A-4GFP: n=35. Mid1^{nsm}6Ala-S42A-S67A-4GFP: n=56. **H:** Percentage of misplaced septa. Cells were grown at 30°C. Error bars: SD, 6 independent counts of 100 cells.

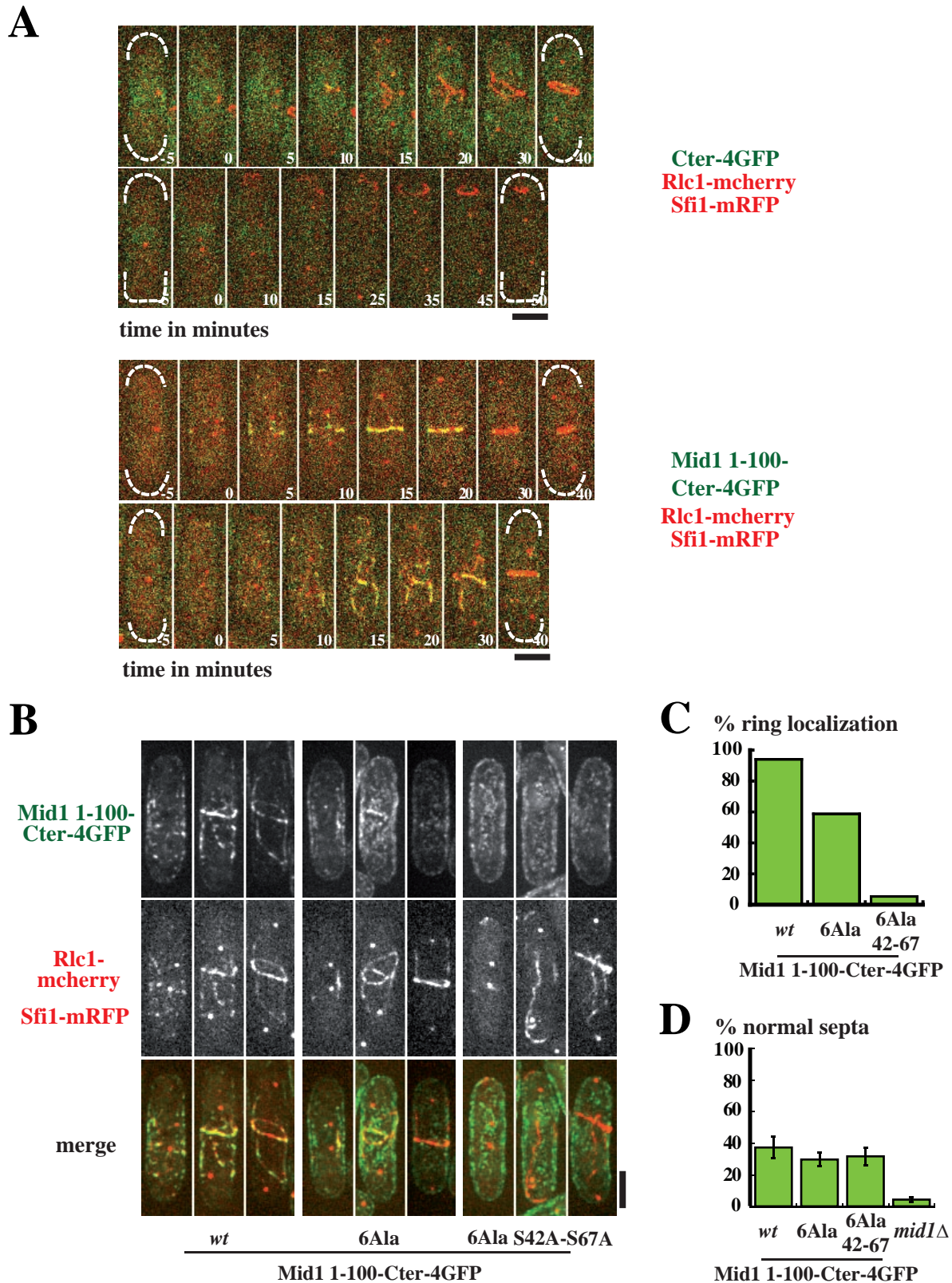


Figure S4: Functional analysis of Mid1 1-100-Cter, Mid1 1-100-6Ala-Cter and Mid1 1-100-6Ala-S42A-S67A-Cter . A: Time-lapse movies of *mid1*Δ cells expressing Cter-4GFP (top) or Mid1 1-100-Cter-4GFP (bottom), Rlc1-mcherry and SPB component Sfi1-mRFP. Mid1 is shown in green and Rlc1 and Sfi1 in red. Time is in minutes. Time 0: SPB separation. Bar: 4 μm. **B:** Localization of Mid1 1-100-Cter-4GFP (left), Mid1 1-100-6Ala-Cter-4GFP (middle) and Mid1 1-100-6Ala-S42A-S67A-Cter-4GFP (right) during mitosis in cells deleted for *mid1* expressing Rlc1-mcherry and Sfi1-mRFP. Maximum projections of z stacks. Bar: 4 μm. Mid1 1-100-6Ala-S42A-S67A-Cter-4GFP also contains a mutation in Mid1 C-terminal NLS which does not alter the functionality of Mid1 1-100-Cter (not shown). **C:** Percentage of mitotic cells with colocalization of Mid1 1-100-Cter-4GFP (n=83), Mid1 1-100-6Ala-Cter-4GFP (n=58) or Mid1 1-100-6Ala-S42A-S67A-Cter-4GFP (n=56) with Rlc1-mcherry filaments before septation onset. **D:** Percentage of normally placed septa of same cells as in B and *mid1*Δ cells. Cells were grown at 30°C. Error bars: SD, 6 independent counts of 100 cells.

Table S1. Table of Strains Used in This Study

Strain	Genotype	Source or Reference
AP240	<i>ade6-M210 leu1-32 ura4-D18 h-</i>	Laboratory collection
AP241	<i>ade6-M216 leu1-32 ura4-D18 h+</i>	Laboratory collection
AP527	<i>mid1::ura4+ ade6-M216 leu1-32 ura4-D18 h- + pAP146 (pmid1-mid1-GFP, leu1+) integrated</i>	Laboratory collection
AP621	<i>mid1::ura4+ ade6-M216 leu1-32 ura4-D18 h- + pAP144 (pmid1-Ctermid1-GFP, leu1+) integrated</i>	Celton-Morizur et al, 2004
AP998	<i>mid1::ura4+ ade6-M216 leu1-32 ura4-D18 h- + pSM26 (pmid1-GFP-Ntermid1, leu1+) integrated</i>	Celton-Morizur et al, 2004
AP1072	<i>mid1::KanMX4 ade6-M216 leu1-32 ura4-D18 h-</i>	Celton-Morizur et al, 2004
AP1324	<i>mid1::ura4+ ade6-M216 leu1-32 ura4-D18 h- + pSM64(pmid1-mid1-T517A-GFP, leu1+) integrated</i>	This study
AP1399	<i>mid1::ura4+ ade6-M216 leu1-32 ura4-D18 h- + pSM81(pmid1-Ctermid1-T517A-GFP, leu1+) integrated</i>	This study
AP1555	<i>mid1::KanMX4 ade6-M216 leu1-32 ura4-D18 h- + pAP146 integrated h- + pAP190 (pnmt-plo1, ura4+)</i>	This study
AP1564	<i>mid1::KanMX4 ade6-M216 leu1-32 ura4-D18 h- + pAP144 integrated h- + pAP190</i>	This study
AP1568	<i>mid1::KanMX4 ade6-M216 leu1-32 ura4-D18 h- + pSM26 integrated h- + pAP190</i>	This study
AP1775	<i>mid1::ura4+ ade6-M216 leu1-32 ura4-D18 h- + pMA7 (pmid1-GFP-Ntermid1Δ250-300, leu1+) integrated</i>	This study
AP1776	<i>mid1::ura4+ ade6-M216 leu1-32 ura4-D18 h- + pMA2 (pmid1-GFP-Ntermid1Δ1-50, leu1+) integrated</i>	This study
AP1778	<i>mid1::ura4+ ade6-M216 leu1-32 ura4-D18 h- + pMA3 (pmid1-GFP-Ntermid1Δ450-506, leu1+) integrated</i>	Almonacid et al, 2009
AP1786	<i>mid1::ura4+ ade6-M216 leu1-32 ura4-D18 h- + pMA6 (pmid1-GFP-Ntermid1Δ200-250, leu1+) integrated</i>	This study
AP1789	<i>mid1::ura4+ ade6-M216 leu1-32 ura4-D18 h- + pMA8 (pmid1-GFP-Ntermid1Δ350-400, leu1+) integrated</i>	This study
AP1792	<i>mid1::ura4+ ade6-M216 leu1-32 ura4-D18 h- + pMA9 (pmid1-GFP-Ntermid1Δ400-450, leu1+) integrated</i>	Almonacid et al, 2009
AP1798	<i>mid1::ura4+ ade6-M216 leu1-32 ura4-D18 h- + pMA4 (pmid1-GFP-Ntermid1Δ150-200, leu1+) integrated</i>	This study
AP1801	<i>mid1::ura4+ ade6-M216 leu1-32 ura4-D18 h- + pMA11 (pmid1-GFP-Ntermid1Δ50-100, leu1+) integrated</i>	This study
AP1804	<i>mid1::ura4+ ade6-M216 leu1-32 ura4-D18 h- + pMA5 (pmid1-GFP-Ntermid1Δ100-150, leu1+) integrated</i>	This study
AP1805	<i>mid1::ura4+ ade6-M216 leu1-32 ura4-D18 h- + pMA10 (pmid1-GFP-Ntermid1Δ300-350, leu1+) integrated</i>	Almonacid et al, 2009
AP1919	<i>mid1::KanMX4 ade6-M216 leu1-32 ura4-D18 h- + pMA11 integrated + pAP190</i>	This study
AP1960	<i>mid1::KanMX4 ade6-M216 leu1-32 ura4-D18 h- + pSM26 integrated + pAP190</i>	This study
AP1962	<i>mid1::KanMX4 ade6-M216 leu1-32 ura4-D18 h- + pMA2 integrated + pAP190</i>	This study
AP2003	<i>mid1::KanMX4 ade6-M216 leu1-32 ura4-D18 h- + pMA25(pmid1-GFP-Ntermid1Δ50-100Δ450-506, leu1+) integrated</i>	This study
AP2005	<i>mid1::KanMX4 ade6-M216 leu1-32 ura4-D18 h- + pMA26 (pmid1-mid1^{nsm}-4GFP, leu1+) integrated</i>	Almonacid et al, 2009
AP2007	<i>mid1::KanMX4 ade6-M216 leu1-32 ura4-D18 h- + pMA31(pmid1-mid1^{nsm}Δ50-100-4GFP, leu1+) integrated</i>	This study
AP2049	<i>mid1::ura4+ ade6-M216 leu1-32 ura4-D18 h- + pMA35 (pmid1-mid1^{nsm}Δ50-100,</i>	This study

	<i>leu1+</i>) integrated	
AP2273	<i>mid1::ura4+ ade6-M216 leu1-32 ura4-D18 h- + pMA49(pmid1-mid1^{nsm}, leu1+) integrated</i>	Almonacid et al, 2009
AP2331	<i>mid1::ura4+ rlc1-mcherry::natR Sfi1-mRFP::kanMX6 leu1-32 ura4-D18 h- + pMA26 integrated</i>	This study
AP2355	<i>mid1::ura4+ rlc1-mcherry::natR Sfi1-mRFP::kanMX6 ade6-M216 leu1-32 ura4-D18 h+ + pMA31 integrated</i>	This study
AP2359	<i>mid1::KanMX4 ade6-M216 leu1-32 ura4-D18 h- + pMA52 (pmid1-mid1-6Ala-4GFP, leu1+) integrated</i>	This study
AP2416	<i>mid1::ura4+ rlc1-mcherry::natR Sfi1-mRFP::kanMX6 ade6-M216 leu1-32 ura4-D18 h- + pMA52 integrated</i>	This study
AP2433	<i>mid1::KanMX4 ade6-M216 leu1-32 ura4-D18 h- + pMA25 integrated+pAP190</i>	This study
AP2436	<i>mid1::ura4+ ade6-M216 ura4-D18 h- + pAM21 (pmid-mid1-T517A-12myc, leu1+) integrated</i>	This study
AP2437	<i>mid1::ura4+ ade6-M216 ura4-D18 h- + pAM22 (pmid-mid1-12myc, leu1+) integrated</i>	This study
AP2441	<i>mid1::KanMX4 ade6-M216 leu1-32 ura4-D18 h- + pMA58(pmid1-mid1^{nsm}6Ala-4GFP, leu1+) integrated</i>	This study
AP2482	<i>mid1::ura4+ rlc1-mcherry::natR Sfi1-mRFP::kanMX6 ade6-M216 leu1-32 ura4-D18 h+ + pMA58 integrated</i>	This study
AP2586	<i>mid1::ura4+ rlc1-mcherry::natR Sfi1-mRFP::kanMX6 leu1-32 ura4-D18 h+</i>	This study
AP2643	<i>nda3-KM311 mid1::KanMX4 ade6-M216 leu1-32 ura4-D18 h+ + pMA66(pmid1-mid1-6Ala-GFP, leu1+) integrated</i>	This study
AP2647	<i>nda3-KM311 mid1::KanMX4 ade6-M216 leu1-32 ura4-D18 h+ + pMA68(pmid1-mid1-GFP, leu1+) integrated</i>	This study
AP2649	<i>nda3-KM311 mid1::KanMX4 ade6-M216 leu1-32 ura4-D18 h+ + pMA69(pmid1-GFP-mid1, leu1+) integrated</i>	This study
AP2738	<i>mid1::KanMX4 ade6-M216 leu1-32 ura4-D18 h+ + pMA65 integrated (pmid1-mid1-6Ala, leu1+)</i>	This study
AP2739	<i>mid1::KanMX4 ade6-M216 leu1-32 ura4-D18 h+ + pMA66 integrated</i>	This study
AP2740	<i>mid1::KanMX4 ade6-M216 leu1-32 ura4-D18 h- + pMA68 integrated</i>	This study
AP2742	<i>mid1::KanMX4 ade6-M216 leu1-32 ura4-D18 h+ + pMA66 integrated + pAP190</i>	This study
AP2743	<i>mid1::KanMX4 ade6-M216 leu1-32 ura4-D18 h- + pMA68 integrated + pAP190</i>	This study
AP2807	<i>mid1::ura4+ rlc1-mcherry::natR Sfi1-mRFP::kanMX6 leu1-32 ura4-D18 h+ + pMA83 (pmid1-mid1-1-100-Cter-4GFP, leu1+) integrated</i>	This study
AP2808	<i>mid1::ura4+ rlc1-mcherry::natR Sfi1-mRFP::kanMX6 leu1-32 ura4-D18 h+ + pMA87 (pmid1-Ctermid1-4GFP, leu1+) integrated</i>	This study
AP2840	<i>mid1::ura4+ plo1-gfp::kanMX6 ade6M216 leu1-32 ura4?+ h- +pAM21 integrated</i>	This study
AP2842	<i>mid1::ura4+ plo1-gfp::kanMX6 ade6M216 leu1-32 ura4?+ h- +pAM22 integrated</i>	This study
AP2925	<i>mid1::ura4+ rlc1-mcherry::natR Sfi1-mRFP::kanMX6 leu1-32 ura4-D18 ade6-M216 h- + pSM64 integrated</i>	This study
AP2927	<i>mid1::ura4+ rlc1-mcherry::natR Sfi1-mRFP::kanMX6 leu1-32 ura4-D18 h- + pAP146 integrated</i>	This study
AP2961	<i>mid1::ura4+ ade6-M216 leu1-32 ura4-D18 h- + pMG20 (pmid-mid1^{nsm}6Ala, leu1+) integrated</i>	This study
AP2966	<i>plo1-gfp::kan mid1::ura4+ ade6M216 leu1-32 ura4? h-</i>	This study
AP2967	<i>plo1-gfp::kan mid1::ura4+ ade6M216 leu1-32 ura4? h- + pMA89 integrated (pmid - mid1Δ507-625-12myc, leu1+)</i>	This study
AP2968	<i>plo1-gfp::kan mid1::ura4+ ade6M216 leu1-32 ura4? h- + pMA91 (pmid-Ctermid1-12myc, leu1+) integrated</i>	This study
AP2969	<i>plo1-gfp::kan mid1::ura4+ ade6M216 leu1-32 ura4? h- + pMA119 (pmid-mid1Δ626-920-12myc, leu1+) integrated</i>	This study
AP2970	<i>plo1-gfp::kan mid1::ura4+ ade6M216 leu1-32 ura4? h- + pMA121 (pmid-mid1ΔRQSTPV-12myc, leu1+) integrated</i>	This study

AP2972	<i>plo1-gfp::kan mid1::ura4+ ade6M216 leu1-32 ura4? h- + pAP97 integrated (pmid- Ntermid1 leu1+)</i>	This study
AP2973	<i>plo1-gfp::kan mid1::ura4+ ade6M216 leu1-32 ura4? h+ + pMA67 integrated (pmid-mid1, leu1+)</i>	This study
AP2982	<i>mid1::ura4+ rlc1-mcherry::natR Sfi1-mRFP::kanMX6 leu1-32 ura4-D18 h+ +pMA115 (pmid-mid1-1-100-6Ala-Cter-4GFP, leu1+) integrated</i>	This study
AP2986	<i>mid1::ura4+ rlc1-mcherry::natR Sfi1-mRFP::kanMX6 leu1-32 ura4-D18 h+ +pMA129 (pmid-mid1^{nsM}6ala-T517A-4GFP, leu1+) integrated</i>	This study
AP2990	<i>mid1::ura4+ rlc1-mcherry::natR Sfi1-mRFP::kanMX6 leu1-32 ura4-D18 h+ + pMA141 (pmid-mid1^{nsM}6Ala-S42A-S67A -4GFP, leu1+) integrated</i>	This study
AP2991	<i>mid1::ura4+ rlc1-mcherry::natR Sfi1-mRFP::kanMX6 leu1-32 ura4-D18 h+ +pMA150 (pmid-mid1-1-100-6Ala-S42A-S67A-CterNLS*-4GFP, leu1+) integrated</i>	This study
AP3167	<i>mid1::ura4+ rlc1-mcherry::natR Sfi1-mRFP::kanMX6 leu1-32 ura4-D18 ade6-M216 +pAP221 integrated h-</i>	This study
AP3178	<i>mid1::ura4+ plo1-gfp::kanMX6 rlc1-mcherry::natR ade6-M216 leu1-32 ura4? h- +pAM21 integrated</i>	This study
AP3179	<i>mid1::ura4+ plo1-gfp::kanMX6 rlc1-mcherry::natR ade6-M216 leu1-32 ura4? h- +pAM22 integrated</i>	This study

Table S2. List of Relevant Phosphopeptides Detected by Mass Spectrometry Analysis of GFP-Mid1 Purified from Mitotic Cell Extracts

Peptide
GLENpS ²⁴ FLSSPNR
EKpT ³⁴ PLFFEGNSNETSGYDQTK
TPLFFEGNpS ⁴² NETSGYDQTK
TPLFFEGNSNETpS ⁴⁶ GYDQTK
KNFTHGDGDM _{ox} pS ⁶² LGNLpS ⁶⁷ ELNVA
SMYMHGYGHLDS ⁹⁴ S ⁹⁵ FS ⁹⁷ S ⁹⁸ QHSPDNR
AEIpS ⁵⁰⁷ ASIDELRQSpT ⁵¹⁷ PV

See also <http://xfer.curie.fr/get/MBbZulJQKw5/MS2SpectraInvivo1.pdf> and <http://xfer.curie.fr/get/mXW1P6FI5Qv/MS2SpectraInvivo2.pdf> for spectra

Table S3. List of Relevant Phosphopeptides Detected by Mass Spectrometry Analysis of Mid1 GST-Nter Phosphorylated In Vitro by Plo1

Peptide
GLENpS ²⁴ FLSSPNR
EKpT ³⁴ PLFFEGNSNETSGYDQTK
TPLFFEGNSNETpS ⁴⁶ GYDQTK

See also <http://xfer.curie.fr/get/r4ERQBmRlG/MS2SpectraInvitro.pdf> for spectra

Supplemental Experimental Procedures

Yeast Genetics, Strains and Plasmids

All *S. pombe* strains are isogenic to 972 and listed in Supplementary Table S1. Standard *S. pombe* molecular genetics techniques and media were used (http://www.sanger.ac.uk/PostGenomics/S_pombe/docs/nurse_lab_manual.pdf).

The plasmids used in this study derive from integrative vector pJK148 [1] or from pSGP572 (generous gift from S. Forsburg). Plasmids pAP97, pAP144, pAP146 and pSM26 were described previously [2, 3] as well as pMA3, pMA9, pMA10, pMA26 and pMA49[4].

For pAP190, a NdeI-SacI fragment from pREP1-plo1 (pDM118, generous gift from D. McCollum) was subcloned into XhoI -SacI digested pSGP572.

For pSM64, a BglII-XbaI fragment of pSM54 carrying T517A mutation obtained by site-directed mutagenesis on pAP32 [3] was subcloned into BglII-XbaI digested pAP146. pSM81 (pmid-Cter-T517A-GFP) was obtained in several steps by subcloning of a XhoI-PstI fragment amplified by PCR from pSM54 containing a 5' fragment of Mid1 Cter and T517A, a PstI-SmaI fragment containing the 3' fragment of Mid1 Cter and GFP and a SmaI-SacI fragment containing nmt1 stop into SalI-SacI digested pAP140 carrying mid1 promoter. To obtain pAM21 and pAM22, a NotI-SacI fragment from pINV-myc (Iakovoni et al., 1999; generous gift from P. Russell) carrying a 12myc tag and nmt1 stop was cloned into NotI-SacI digested pSM64 and pAP146 respectively.

To produce plasmids pMA2, pMA4, pMA5, pMA6, pMA7, pMA8, and pMA11, NotI-BamHI fragments carrying 150 bp long deletions within mid1 N-terminus sequence were obtained by double PCR using pSM26 as a template and subcloned into pSM26 digested with the same enzymes. To obtain pMA22, a SalI-SpeI PCR fragment encoding Mid1 N-Terminus carrying deletion of aa 50-100 and a SpeI-SalI fragment encoding Mid1 C-terminus were cloned into pMA12 [4] digested by SalI. To produce pMA25, a BsmI-BsmI fragment of pMA11 carrying Mid1 promoter and deletion of aa 50-100 was cloned into BsmI-BsmI digested pMA3. pMA31 was obtained by subcloning a BsmI-BsmI fragment from pMA22 containing Mid1 promoter and deletion of aa 50-100 into BsmI-BsmI digested pMA26 containing the nsm mutation. pMA35 was obtained by cloning an XbaI-SacI fragment of pAP32 [3] into XbaI-SacI digested pMA31. pMA50 and pMA51 were obtained by introducing S95A mutation and S15A and S24A mutations respectively on pMA47 (pmid1-mid1T34A S46A S62A-4GFP). pMA52 was obtained by subcloning an AvrII-NotI fragment of pMA50 carrying mutations T34A, S46A, S62A and S95A into AvrII-NotI digested pMA51 carrying mutations S15A and S24A and 4GFP tag. To obtain pMA58, a pMA52 BsmI-BsmI fragment carrying Mid1 promoter and the 6Ala mutations and a pMA26 BsmI-NotI fragment carrying the nsm mutation were subcloned into NotI-BsmI digested pMA26. pMA65 and pMA66 were obtained by subcloning an XcmI-SacI fragment of pAP32 and pAP146 respectively into XcmI-SacI digested pMA52. To obtain pMA68, a XcmI-SacI fragment of pAP146 was cloned into XcmI-SacI digested pAP221 [5] and pMA69 was obtained by subcloning a SalI-SacI fragment from pAP70 (pnmt-GFP-mid1) into XhoI-SacI digested pAP140 [2]. To obtain pMA83, a SalI-SpeI digested PCR fragment corresponding to Mid1 aa 1-100 and a SpeI-SacI fragment of pMA24 [4] containing Mid1 Cter were subcloned into SalI-SacI digested pAP140. pMA87 was obtained by subcloning an XcmI-SacI fragment from pAP221 into XcmI-SacI digested pAP144. pMA89 and pMA91 were obtained by

subcloning a XcmI-SacI fragment from pAM21 into XcmI-SacI digested pSM1 derived from pAP146 and carrying a Mid1 Δ 506-625 construct produced by double PCR, or pMA87. To obtain pMA115, a SalI-SpeI digested PCR fragment corresponding to Mid1 aa 1-100 carrying mutations S15A, S24A, T34A, S46A, S62A and S95A and a SpeI-SacI fragment of pMA24 containing Mid1 Cter and the 4GFP tag were subcloned into SalI-SacI digested pAP140. pMA119 was obtained by subcloning a BglII-NotI digested PCR fragment encoding Mid1 aa 1-625 into BglII-NotI digested pAM22. To obtain pMA121, deletion of RQSTPV sequence was introduced between a KpnI-NheI Nter and a NheI-NotI Cter PCR fragment, subcloned into KpnI-NotI digested pAM22. pMA129 was obtained by subcloning a SpeI-SfoI digested PCR fragment containing T517A mutation into SpeI-SfoI digested pMA58. To obtain pMA141, S42A mutation was first introduced on pMA58 by site-directed mutagenesis to produce pMA95. Then, a KpnI-BglII digested PCR fragment from pMA95 with additional S67A mutation was subcloned into KpnI-BglII digested pMA58. To produce pMA150, a KpnI-SpeI digested PCR fragment from pMA141 corresponding to Mid1 promoter and Mid1 aa 1-100 carrying mutations S15A, S24A, T34A, S42A, S46A, S62A, S67A and S95A was subcloned into KpnI-SpeI digested pMA58. pMG20 was produced by subcloning a XcmI-SacI fragment from pAP32 into pMA58.

For in vitro production of Plo1 polo box domain (PBD; aa331-683), PBD sequence was cloned into pMAL-2C (pDC1) between SalI and BamHI sites. To produce Rng2-1306-End fragment, a SalI/EcoRI fragment encoding aa1306-1489 of Rng2 was cloned into pMAL-2C. Mid1 Nter (aa1-422; pKG4014), Mid1 Nter-8Ala (Nter with S7A, S15A, S24A, T34A, S46A, T51A, S62A and S95A mutations; pMA107), Mid1 Cter (aa443-920; pKG4015), Mid1Cter-T517A (Cter with mutation T517A; pKG4557), Mid1 1-100 (aa 1-100; pMA142) and Mid1 1-100-6Ala (aa 1-100 with S15A, S24A, T34A, S46A, S62A, and S95A mutations; pMA143) were cloned into pGEX-2T between SmaI and SalI sites.

All point mutations were introduced by site-directed mutagenesis using Quickchange kit (Stratagene) according to the manufacturer's instructions.

All Mid1 constructs were integrated into the genome of *mid1* Δ *leu1*-32 strains (AP 245, AP1072 [2, 3], AP2586 or AP2966, see TableS1) after linearization by NruI in *leu1* gene. Transformations was performed using Lithium acetate-DMSO method [6].

Plo1-GFP strain was a generous gift from Dan McCollum. Genomic tagging of *sfi1* was performed as described [6] and described previously for *rlc1* [7].

In Vitro Binding Assays with Plo1 PBD and Rng2 1306-End Fragment

Binding assays with recombinant bacterially produced proteins, purified on either glutathione beads (GST) or amylose beads (MBP), were performed as previously described [8], except binding was done in MBP buffer (20 mM Tris-HCl, pH 7.4, 150 mM NaCl, 2 mM EDTA, and 0.1% Triton X-100). Proteins were resolved by SDS-PAGE, followed by Coomassie blue staining or Western blot analysis with anti-MBP (Abcam) to visualize proteins.

Cdc2 and Plol Kinase Assays on Recombinant Mid1 Nter and Cter

Approximately 50 ng of recombinant HA-Cdc2-His₆-Cdc13 or HA-Cdc2^{kd}-His₆-Cdc13 complex, purified from baculovirus infected *Sf9* cells as described [9], was used to phosphorylate 1 µg of recombinant Mid1 GST-Nter, Mid1 GST-Cter or Mid1 GST-Cter-T517A in HB15 buffer (25mM MOPS, pH 7.2, 60 mM β-glycerophosphate, 15 mM p-nitrophenyl phosphate, 15 mM MgCl₂, 1 mM DTT, 15 mM EGTA) supplemented with 20 µM cold ATP and 5 µCi [γ -³²P]ATP. Reactions were incubated at 30°C for 30 min and terminated by the addition of sample buffer. Samples were boiled and separated on SDS-PAGE. Coomassie staining or autoradiography was used for detection of proteins. Plol kinase was purified from baculovirus infected *Sf9* cells as described for HA-Cdc2-His₆-Cdc13 [9], except cells were treated with 0.1 µM okadaic acid for 4 hr prior to lysis. Plol kinase assays were performed similarly to Cdc2 assays, except reaction buffer consisted of 1 mM Hepes, pH 7.2, 15 mM KCl, 1 mM MgCl₂, 0.2 mM DTT, 0.1 mM EGTA. For mass spectroscopy analysis, kinase assays were performed in the absence of [γ -³²P]ATP but with 1mM cold ATP. Two-dimensional phospho-tryptic peptide mapping was performed as described in [10].

Coimmunoprecipitation Experiments

IPs were performed as described [2]: 100 ml of cells grown at 1x10⁷ cells/ml at 30°C in YE5S were resuspended in 300 µl IP buffer. Extracts were incubated with anti-mouse IgG magnetic beads (M-280 DYNAL, Invitrogen) coupled to 6 µg of anti-GFP mAb (Roche) or anti-HA mAb 12CA5 (Roche). Western blots were performed with anti-GFP mAb (1/500, Roche), anti-Mid1 affinity purified Ab (1/100) and anti-myc mAb 9E10 (1/500, Roche). Secondary Abs were coupled to peroxidase (Jackson Immunoresearch) or to alkaline phosphatase (Promega).

Mass Spectrometry Analysis of Phosphopeptides from Mitotic GFP-Mid1 and Mid1 Nter Phosphorylated In Vitro by Plol

1 l of AP2649 cells were grown at 4x10⁷ cells/ml at 30°C in YE5S medium concentrated 2 times as compared to regular YE5S medium (YE5S2X) and shifted for 7 h at 18°C to block cells in mitosis. Cells were resuspended in 12 ml IP buffer and extracts were incubated with anti-mouse IgG magnetic beads (M-280 DYNAL, Invitrogen) coupled to 12 µg of anti-GFP mAb (Roche). Samples were run for SDS-PAGE on Nupage BisTris gels 10% (Invitrogen).

Standard in gel digestions were performed after colloidal blue (Agro-bio) staining of proteins. Briefly, following washing of the excised gel slice, proteins were reduced by adding DTT (Sigma Aldrich) prior to alkylation with iodoacetamide (Sigma Aldrich). After washing and shrinking of the gel piece with 100% acetonitrile, trypsin (Sequencing Grade Modified, Roche Diagnostics) or elastase (Sigma Aldrich) was added and proteins were digested overnight as previously described [11, 12]. For phosphopeptide analysis probes were directly used for nanoLC-MS/MS. The sample was first separated on a C18 reversed phase column (75 µm i.d. x 15 cm, packed with C18 PepMapTM, 3 µm, 100 Å; LC Packings) via a linear acetonitrile gradient (UltiMate 3000 system; Dionex) before MS and MS/MS spectra were recorded on an LTQ Orbitrap XLTM mass spectrometer (Thermo SCIENTIFIC). The mass spectrometer was set to acquire a single MS scan followed by up to 5 data-dependent scans and, if a neutral loss of 98 Da

from the precursor ion was observed in the CID mass spectrum, an MS3 scan of the neutral loss ion (simultaneous fragmentation of neutral loss product and precursor was enabled, dynamic exclusion repeat count of 1, repeat duration of 30 seconds, exclusion duration of 180 seconds and lock-mass option was enabled). The resulting spectra were then analyzed via the Mascot™ and the SEQUEST® Software (Matrix Science and Thermo Scientific) created with Proteome Discoverer (version: 1.2.0.92, Thermo Scientific) using the NCBI nr *Schizosaccharomyces Pombe* Protein Database. Only phosphorylated peptides which have their non-phosphorylated counterparts were manually validated. All phosphorylated peptides were detected in minimum two different analyses. Mass spectrometric analysis of recombinant GST-Mid1 Nter (1-424) from in vitro Plo1 kinase assays was performed by LC-MS after in gel triple digestion with Trypsin, Chymotrypsin, and Elastase.

Microscopy

Cells were grown exponentially at 25°C in YE5S except for Plo1 overexpression experiments where cells were grown in EMM medium without thiamine with appropriate supplements at 25°C or at room temperature in the case of Mid1 Nter.

Cell walls and septa were stained with Fluostain I (Sigma) on cells grown at 30°C. The percentage of abnormal septa was determined by visual inspection. Abnormal septa include septa not perpendicular to the cell long axis, not dividing the cell equally, misshaped and double septa.

Two microscopy setups were used. For Plo1-GFP (Fig S1C-D), Mid1-517A-GFP localization (Fig S1E), localization of GFP-Nter mutants (Fig 2C), Plo1 overexpression experiments (Fig S2A), Mid1-6Ala-GFP and Mid1-6Ala-4GFP (Fig S2E-F) and Fluostain staining (Fig 4B), we used a DMRXA2 upright Microscope (Leica Microsystems) equipped with a 100X/ 1.4 NA Plan Apochromat objective and a Coolsnap HQ CCD camera (Roper). In this case, 2 µl of cells were mounted directly between slide and coverslip. 2 s exposure (binning 1 gain1) in a single focal plane were used for Mid1 constructs. Plo1-GFP was imaged as 21 stacks of 0,2 µm with 500 ms exposure (binning 1 gain 2, FigS1C) or for 2 s (binning 1 gain1) in a single focal plane (FigS1D).

For all time-lapse movies (3A, S3A-B-E, S4A), for imaging clusters in Mid1 GFP-Nter upon Plo1 overexpression (Fig 2D), Mid1 1-100-Cter-4GFP constructs (Fig 4A, S4B), we used a Nikon Eclipse TE2000-U microscope equipped with a 100X 1.45NA, oil immersion objective, a PIFOC Objective stepper, a Yokogawa CSU22 confocal unit and a Roper HQ2 CCD camera. Cells were mounted directly between slide and coverslip (Fig 2D), on YE5S agarose pads [13] (Fig 4A, S4B) or in PDMS chambers filled with 2% agarose in EMM medium containing appropriate supplements [4] (Fig 3A, S3A-B-E, S4A). For time lapse movies, stacks of 7 planes spaced by 1 µm were acquired every 2 minutes (binning 2 gain 3; 400 ms at 30% laser power for mCherry and 200 ms at 40% for GFP; Fig 3A, S3A-B-E) or every 5 minutes (Fig S4A) using Metamorph software. For GFP-Nter clusters, stacks of 31 planes spaced by 0,2 µm were acquired (binning 2 gain 3; 200 ms at 40% for GFP; Fig 2D). For Mid1 Cter-4GFP and Mid1 1-100-Cter-4GFP constructs, stacks of 7 planes spaced by 1 µm were acquired (binning 2 gain 3; 400 ms at 40% laser power for mCherry and 400 ms at 60% for GFP; Fig 4A, S4B).

Supplemental References

1. Keeney, J.B., and Boeke, J.D. (1994). Efficient targeted integration at *leu1-32* and *ura4-294* in *Schizosaccharomyces pombe*. *Genetics* *136*, 849-856.
2. Celton-Morizur, S., Bordes, N., Fraissier, V., Tran, P.T., and Paoletti, A. (2004). C-terminal anchoring of *mid1p* to membranes stabilizes cytokinetic ring position in early mitosis in fission yeast. *Mol Cell Biol* *24*, 10621-10635.
3. Paoletti, A., and Chang, F. (2000). Analysis of *mid1p*, a protein required for placement of the cell division site, reveals a link between the nucleus and the cell surface in fission yeast. *Mol Biol Cell* *11*, 2757-2773.
4. Almonacid, M., Moseley, J.B., Janvore, J., Mayeux, A., Fraissier, V., Nurse, P., and Paoletti, A. (2009). Spatial control of cytokinesis by *Cdr2* kinase and *Mid1*/anillin nuclear export. *Curr Biol* *19*, 961-966.
5. Celton-Morizur, S., Racine, V., Sibarita, J.B., and Paoletti, A. (2006). *Pom1* kinase links division plane position to cell polarity by regulating *Mid1p* cortical distribution. *J Cell Sci* *119*, 4710-4718.
6. Bahler, J., Wu, J.Q., Longtine, M.S., Shah, N.G., McKenzie, A., 3rd, Steever, A.B., Wach, A., Philippsen, P., and Pringle, J.R. (1998). Heterologous modules for efficient and versatile PCR-based gene targeting in *Schizosaccharomyces pombe*. *Yeast* *14*, 943-951.
7. Moseley, J.B., Mayeux, A., Paoletti, A., and Nurse, P. (2009). A spatial gradient coordinates cell size and mitotic entry in fission yeast. *Nature* *459*, 857-860.
8. Carnahan, R.H., and Gould, K.L. (2003). The PCH family protein, *Cdc15p*, recruits two F-actin nucleation pathways to coordinate cytokinetic actin ring formation in *Schizosaccharomyces pombe*. *J Cell Biol* *162*, 851-862.
9. Yoon, H.J., Feoktistova, A., Wolfe, B.A., Jennings, J.L., Link, A.J., and Gould, K.L. (2002). Proteomics analysis identifies new components of the fission and budding yeast anaphase-promoting complexes. *Curr Biol* *12*, 2048-2054.
10. Ren, L., Feoktistova, A., McDonald, W. H., Den Haese, G., Morrell, J. L. and Gould, K. L. (2005). Analysis of the role of phosphorylation in fission yeast *Cdc13p*/CyclinB function. *J. Biol. Chem.* *280*, 14591-14596.
11. Fevrier, B., Vilette, D., Archer, F., Loew, D., Faigle, W., Vidal, M., Laude, H., and Raposo, G. (2004). Cells release prions in association with exosomes. *Proc Natl Acad Sci U S A* *101*, 9683-9688.
12. Schlosser, A., Bodem, J., Bossemeyer, D., Grummt, I., and Lehmann, W.D. (2002). Identification of protein phosphorylation sites by combination of elastase digestion, immobilized metal affinity chromatography, and quadrupole-time of flight tandem mass spectrometry. *Proteomics* *2*, 911-918.
13. Tran, P.T., Paoletti, A., and Chang, F. (2004). Imaging green fluorescent protein fusions in living fission yeast cells. *Methods* *33*, 220-225.